Halogen Bonding in Iodo-perfluoroalkane/Pyridine Mixtures

Haiyan Fan,[†] Jeffrey K. Eliason,[†] C. Diane Moliva A.,[†] Jason L. Olson,[†] Scott M. Flancher,[‡] M. W. Gealy,[‡] and Darin J. Ulness*,[†]

Department of Chemistry, Concordia College, Moorhead, Minnesota 56562, Department of Physics, Concordia College, Moorhead, Minnesota 56562

Received: June 17, 2009; Revised Manuscript Received: November 7, 2009

Mole fraction and temperature studies of halogen bonding between 1-iodo-perfluorobutane, 1-iodo-perfluorohexane, or 2-iodo-perfluoropropane and pyridine were performed using noisy light-based coherent anti-Stokes Raman scattering ($I^{(2)}$ CARS) spectroscopy. The ring breathing mode of pyridine both is highly sensitive to halogen bonding and provides a strong $I^{(2)}$ CARS signal. As the lone pair electrons from the pyridinyl nitrogen interact with the σ-hole on the iodine from the iodo-perfluoroalkane, the ring breathing mode of pyridine blue-shifts proportionately with the strength of the interaction. The measured blue shift for halogen bonding of pyridine and all three iodo-perfluoroalkanes is comparable to that for hydrogen bonding between pyridine and water. 2-Iodo-perfluoropropane displays thermodynamic behavior that is different from that of the 1-iodo-perfluoroalkanes, which suggests a fundamental difference at the molecular level. A potential explanation of this difference is offered and discussed.

I. Introduction

The attractive interaction (R−X···Y−R) between a halogen (X) and an atom (Y) possessing a lone pair of electrons, called halogen bonding, is currently receiving a great deal of attention in the literature.[1–4] Halogen bonding is the most actively studied subtype of a more general class of noncovalent interaction called σ-hole bonding.[5,6] Recent computational studies have shown that electronegative atoms, such as halogens, and also atoms of groups IV,[7] V,[8,9] and VI[9,10] can have regions of electropositive potential within the electron density on the distal side of the halogen relative to the R−X bond.[3–6] This electropositive area is termed the σ-hole and provides a region of attraction for molecules containing atoms with lone pair electrons. This electropositive σ-hole enables halogens to behave in a manner analogous to the way electropositive hydrogen does in hydrogen bonding. Indeed, there are numerous examples in biology and material science in which hydrogen and halogen bonding compete to determine the ultimate structure of macromolecular complexes.[1–3]

The specific interaction between a halide and a lone-pair-containing atom has been known for almost 150 years, since the characterization of the I_2···NH_3 interaction[11] and subsequent generalization to X_2···NH_3 complexes.[12] Sixty years ago, Hassel's seminal (and Noble Prize winning) work firmly established the idea that halides may serve as acceptors of lone pair electron density.[13–17] Spectroscopic studies investigating the effects of halogen bonding between organic halides (specifically haloforms) and electron donors were performed by Sandorfy in the late 1970s.[18–21] Interestingly, that work foreshadowed the recent application of halogen bonding in biologically important systems with its investigation of the correlation between halogen bond strength and the effectiveness of halogenated anesthetics.[18–21] Meanwhile, crystallographic work by Murray-Rust et.al. was revealing the geometrical aspects of organic halide-based halogen bonding.[22–24] It was found that, similar to hydrogen bonding, the distance between the halogen atom and the electron donor is shorter than the sum of the van der Waals radii, and the bond angle is roughly 180°. The study of halogen bonding has accelerated considerably in the current decade, catalyzed by three major areas: computational chemistry with the work of Politzer et.al.[4,5,7,8,10,25] and Auffinger et.al.,[3] material science with the work of Metrangolo and Resnati et.al.,[2,26–32,43] and biological chemistry with the work of Auffinger et.al.[3]

Computational studies have provided great insight into the electrostatic nature of the halogens.[3–5,8–10,25,33–37] It has been shown that for chlorine, bromine, and iodine, there is a region of electropositive potential on the distal side of the R−X axis (the σ-hole). This is surrounded by an electroneutral ring and, finally, by an electronegative "belt" oriented in a plane perpendicular to the bond axis.[3–6] Although halogen bonding is often described as analogous to hydrogen bonding, the nature of the electrostatic gradient from positive to negative gives a richness to the halogen-based interaction not exhibited by the entirely electropositive hydrogen in hydrogen bonding. The halogen may, therefore, interact with a nucleophile through σ-hole bonding, but it may also interact with an electrophile via its electronegative belt. Indeed, this is consistent with the very recent study by Beuchamp of the boiling points of 86 haloethanes, which considers the C−X···X interaction to be important.[38] Further, the C−X···H−R bond angle for fluorine, which does not have a σ-hole, is 110−180°, but for the heavy halides, which have σ-holes, the C−X···H−R bond angles range from 90° to 130°.[38] This is consistent with the electrophilic hydrogen interacting with the electronegative belt off-angle from the C−X axis.

A particularly useful application of halogen bonding is found in material science.[1,2,26–32,39–44] A key principle here is halogen-bond-driven cocrystallization. Halogen bonding can facilitate the self-assembly formation of macromolecular superstructures and noncovalent polymers.[1,2,30,43] Further, halogen bonding can direct orientation in liquid crystals.[1,42] Metrangolo et.al. very recently synthesized noncovalent halogen-bond-based dendrim-

* Corresponding author. E-mail: ulnessd@cord.edu.
[†] Department of Chemistry.
[‡] Department of Physics.

10.1021/jp9057127
Published on Web 12/02/2009

eric structures.[43] Related to the pyridine/halogen interaction of the current work, Shirman et.al., in 2008 investigated self-halogen-bond-driven formation of supramolecular assemblies of phenylethenyl pyridine derivatives, in which the nitrogen in the pyridine moiety interacted with a halogen on the phenyl moiety.[44]

The utility and ubiquity of hydrogen bonding in biological systems and the similarity of halogen bonding to hydrogen bonding offers the exciting prospect of exploiting halogen bonding in drug design and molecular biological engineering.[3,45–51] Indeed, the halogen bonding between iodine on the thyroid prohormone thyroxine and its various transport proteins is an example where nature has utilized halogen bonding.[3] Very recently, Voth et al. examined the competition between hydrogen bonding and bromine-based halogen bonding in DNA Halliday junctions using brominated uracil.[45] They report a roughly 2 kcal/mol increase in the stability of the DNA construct with the halogen bond as compared to the natural hydrogen bond construct.[45] This leads to the proposition of halogen bonding as a general tool for biomolecular engineering. In addition, while modeling DNA, Tawarade, Seio, and Sekine synthesized several iodinated nucleosides and investigated the halogen bond interaction between the iodine placed on the aromatic ring and the nitrogen of the pyridinyl moiety on a complementary nucleoside.[46] Just this year, Lu et.al. have investigated halogen-bonding-based ligand/protein binding and suggested halogen bonding could become an important tool in drug design.[47] Also this year, Liu et.al. performed both X-ray-scattering and ligand-binding experiments to study the binding of a number of halogenated benzene compounds within a cavity in bacteriophage T4 lysozyme.[48] They found direct evidence for halogen bonding between iodinated benzene (especially for IC_6H_5) compounds and both sulfur and selenium.

The results of the present work contribute a spectroscopic study of the effect of halogen bonding of several iodo-perfluoroalkanes (C_xF_yI) on the ring breathing mode of pyridine. It has been shown that this mode of pyridine can be a good marker for hydrogen bonding[52–58] because the electron density of the lone pair electrons on the pyridinyl nitrogen participates in the hydrogen bond. Thus, the electronic structure of pyridine is perturbed. This results in a blue shift of the ring breathing frequency.[52–58] In addition, the ring breathing mode of pyridine provides a very strong coherent anti-Stokes Raman scattering (CARS) signal that is exploited in the noisy light CARS method, called $I^{(2)}$ CARS,[59–71] used here. Because of the similarities between hydrogen and halogen bonding, the $I^{(2)}$ CARS method shows a similar blue shifting of the ring breathing mode of pyridine upon halogen bonding as seen in hydrogen bonding. The blue-shift measurements are helpful in sorting out the various thermodynamic contributions to the overall halogen bonding process because it isolates the halogen bond interaction itself. In the liquid state, the free energy for halogen bonding is determined by a number of factors beyond simply the enthalpy for complexation of the halogen bond donor and acceptor. The magnitude of the frequency blue shift directly probes this enthalpy for complexation, so when combined with temperature dependence of the equilibrium constant data that is determined by the overall free energy, one can gain deeper insight into the molecular level structure and dynamics of halogen bond formation.

The tremendous electron-withdrawing power of the fluorine atoms on the alkane backbone give rise to a particularly strong σ-hole on the lone iodine in iodo-perfluoroalkanes. Indeed, the results of this work suggest that halogen bonding of these molecules with pyridine is comparable in strength to the hydrogen bonding of pyridine with water and alcohols.

Not only do iodo-perfluoroalkanes provide a good halogen donor for this study, they are of great importance in crystal engineering precisely because of their strong σ-hole bonding potential. Di-iodinated versions of the molecules studied here are often used in crystal engineering as linkers.[1,2,30] Additionally, but less related to σ-hole bonding, iodo-perfluoroalkanes are key components in the synthesis of ligand systems for organic/fluorinated biphasic catalysis.[72–74] These iodo-perfluoroalkane compounds serve as precursors for fluorinated pony tails that modulate the relative solvation of ligands in organic versus fluorinated phases.[72–74]

II. The σ-Hole

It is important to review the basis for the formation of the σ-hole (and subsequent σ-hole bonding). In a neutral, free halogen atom, the diffuse nature of the electron density relative to localized, positive nuclear charge leads to a net electropositive charge on an arbitrary spherical surface encompassing the atom. As the free atom bonds to a molecule, electron density is directed into the bond region. The degree to which this happens depends on the electron-withdrawing nature of the rest of the molecule and on the polarizability of the halide atom. As the electron density is directed into the bond, the electropositive nature of the halide distal to the bond is enhanced.

Taking a closer look at the substructure of the electron density of the halide using a simple VSEPR/hybridized orbital model, one sees that the degree of hybridization of the atomic orbitals influences the redistribution of the electron density and the degree of increase in the electropositivity of the distal side of the halide in the bond (the strength of the σ-hole). Natural bond orbital (NBO) analysis[75] is a computational method that can assign the percentage of s and p character of a given orbital. Through NBO analysis, it is found that fluorine has a much greater sp hybridization than do the heavy halides.[5] In particular, for iodine and bromine, lone pair electrons are in orbitals that are over 90% s character, as compared to 75% s character for fluorine. Likewise, bonding electrons are in an orbital that has over 90% p character for iodine and bromine but only 75% p character for fluorine. The electron density in the 90% p-based bonding orbital shifts into the bond region. This partially vacates the distal lobe of the p orbital directed along the bond axis and exposes the positive nuclear charge. Although the remaining lone pair electrons in the primarily s character orbitals contribute electron density spherically, the net result is what is now described as the electropositive σ-hole surrounded by a neutral ring and encompassed by an electronegative "belt" of electron density. Very recent work by Murray and Politzer showed that although σ-holes tend to form when the bonding orbital has high p character, as described above, σ-holes can occur on atoms where the bonding orbital has significant s character.[7]

Iodine and bromine form the strongest σ-holes, followed by chlorine. Fluorine does not form a significant σ-hole. The strength of the σ-hole is influenced by the bond orbital character of the atom directly bonded to the halogen. For example, it is observed that sp hybridized carbons lead to strong σ-holes followed by sp^2 and then sp^3 hybridized carbons.[2]

In addition to the strength of the σ-hole, the ultimate strength of the σ-hole bond itself is determined by other factors, as well. As expected, the (Lewis) basicity of the nucleophile is an important factor. For halogen bonding between organics, one often sees nitrogen involved in stronger halogen bonding than oxygen and sulfur.[2] The degree of steric hindrance is, of course,

also important. Because of the size of the halogen atom, steric factors are more important in halogen bonding than in hydrogen bonding.

III. Experiment

The $I^{(2)}$ CARS experiments were performed as described in the literature.[66–68] The noisy light source was a modified pumped dye laser (Spectra Physics) containing rhodamine 640 (Exciton). In this pumped dye laser, the entire lasing spectrum of the dye is emitted in a phase-incoherent way because the frequency selective grating is replaced by a simple mirror. The phase incoherence gives rise to a stochastic electromagnetic field that has a coherence time of ~150 fs, despite its nearly 10 ns pulse duration. A second pumped dye laser (Spectra Physics) containing DCM (Exciton) was used as the narrowband source, M, via normal operation. Both dye lasers were pumped at 10 Hz by a single Nd:YAG laser (Spectra Physics) frequency-doubled to operate at 532 nm.

A Michelson interferometer was used to split the noisy light into twin beams, B and B′. The length of one arm of the interferometer could be changed via a stepper motor (Newport), which was calibrated using the well characterized $I^{(2)}$ CARS signal from benzene.[59,62,66,68] The twin noisy beams emerged from the interferometer running parallel to one another with a separation of ~2 mm on-center. The narrowband beam was made to propagate parallel to the noisy beams in the standard BOX beam configuration. The three beams were focused onto the sample using a 150 mm focal length lens. The beam energies at the sample were on the order of tens of microJoules per pulse. The visually apparent $I^{(2)}$ CARS signal emerged along its own wavevector and was spatially isolated using an iris. The signal was then directed into a monochromator (SPEX) and ultimately onto a 100 × 1340 pixel array, liquid-nitrogen-cooled CCD detector (Roper Scientific/Princeton Instruments). The spectral dimension of the experiment was calibrated using neon lines. The absolute resolution of the spectrometer, as characterized by the half-width at half-maximum of the neon lines, was found to be 0.38 cm^{-1}. $I^{(2)}$ CARS spectra were collected at each delay setting to produce the spectrogram. All spectrograms were produced by moving the stepper motor over a range from −1.00 to 1.00 mm in steps of 0.01 mm. At each delay, a 10-shot average spectrum was recorded. Three to five complete spectrograms were averaged for each sample. Each spectrogram took ~8 min to acquire.

All samples (pyridine, 1-iodo-perfluorobutane, 1-iodo-perfluorohexane, 2-iodo-perfluoropropane, 1-bromo-perfluorohexane) were used as received with no further purification. Mole fraction mixtures, of approximately 1 mL total volume, were created using 1 mL volumetric pipets. The error in mole fraction is estimated to be <1%. Temperature control of the samples was performed using a home-built brass jacket and a recirculating bath (FTS Systems). The temperature was held constant to within ±0.2 °C. During the experiment, the samples were contained in a 2 mm glass cuvette (Starna) with a Teflon stopper. Despite the stopper, a small amount of evaporation of the sample was noted at high temperatures. The operating assumption was that this evaporation did not significantly change the mole fractions of the components in the solution over the duration of the data acquisition runs.

IV. Overview of Theory and Data Analysis

The analytic results for the $I^{(2)}$ CARS signal intensity, $I(\omega_D, \tau)$, as a function of detected frequency (ω_D) and interferometric delay time (τ) are presented here. The material response function is taken to decay exponentially (Lorentzian line shape). An important property $I^{(2)}$ CARS exhibits is that signals from individual Raman active modes within the sample simply add. There is no quantum beating between the signals from different modes. For the component of the signal from a given mode, the frequency and delay-time dependent $I^{(2)}$ CARS signal intensity is approximately given by

$$I(\omega_D, \tau) \propto J(\omega_D) e^{-2\gamma|\tau|}\left(\frac{\cos(\Delta_{CARS}\tau)}{2\gamma}\right) + \frac{R}{2\gamma} e^{-2\gamma|\tau|} \sin(\Delta_{CARS}|\tau|) + I(\omega, \infty) \quad (1)$$

where $I(\omega_D,\infty)$ is the τ-independent background term. In this expression, $J(\omega_D)$ is the spectral density of the broadband light, and R is the nonresonant-to-resonant ratio of the orientationally averaged third-order hyperpolarizabilities.[63] γ is the observed dephasing rate constant, and $\Delta_{CARS} \equiv 2\omega_R + \omega_M - \omega_D$, where ω_M is the frequency of the narrowband beam and ω_D is the detected frequency. The frequency Δ_{CARS} vanishes at the zero difference frequency,[69–71] ω_D^0; here, $\omega_R = (\omega_D^0 - \omega_M)/2$ gives the precise Raman vibrational frequency.

The $I^{(2)}$ CARS spectrograms for each of the pyridine and iodoperfluoroalkane mixtures were fit to eq 1 using Mathematica, which employs the Marquardt−Levenberg version of nonlinear least-squares regression.[76,77]

As mentioned earlier, data are collected in the form of a spectrogram. When Fourier-transformed from time−frequency dimensions to frequency−frequency dimensions, the spectrogram method of detection provides a valuable visual representation of the signal.[57,58,71] The visually apparent x pattern in the transformed spectrogram allows one to unambiguously see Raman modes that are not evident in the raw spectrogram nor would be strongly present in a spectrum representation. Nevertheless, it is difficult to compare one transformed spectrogram to another in anything other than a very gross qualitative way.

Therefore, one additionally compresses the visual information carried by the two-dimensional picture of the Fourier-transformed spectrogram by computing what is called the x-marginal spectrum.[57,58,71] The resulting x-marginal spectrum is comparable to a standard CARS spectrum. It is important to keep in mind, however, that the x-marginal spectra do not provide precise quantitative data regarding the parameters of the material model. Quantitative data are obtained from fitting the spectrograms themselves. The x-marginal spectra simply provide a concise, qualitative representation of the data contained in the spectrograms.

V. Results

The x-marginal spectra for nine different mole fraction values spanning from neat pyridine to $X_{py} = 0.2$ are shown for separate binary mixtures of pyridine with 1-iodo-perfluorobutane, 1-iodo-perfluorohexane, or 2-iodo-perfluoropropane in Figures 1, 2, and 3 respectively. These data were collected at 20 °C. A clear peak begins to emerge at approximately $X_{py} = 0.8$ for each binary system and persists with further addition of the diluent. This peak is from the ring breathing mode of pyridine within the pyridine/iodo-perfluoroalkane halogen bonded complex. Fitting the raw spectrogram data to the multimode version of eq 1 reveals the new peak shifted to the blue by ~7.8, 7.6, or 9.7 cm^{-1} for 1-iodo-perfluorobutane, 1-iodo-perfluorohexane, or 2-iodo-perfluoropropane, respectively. All shifts are reported for $X_{py} = 0.5$ and $T = 20$ °C. These shifts are comparable to those seen for the hydrogen bond complex of pyridine with water or alcohols.[52–58] As with hydrogen bonding, the triangle mode

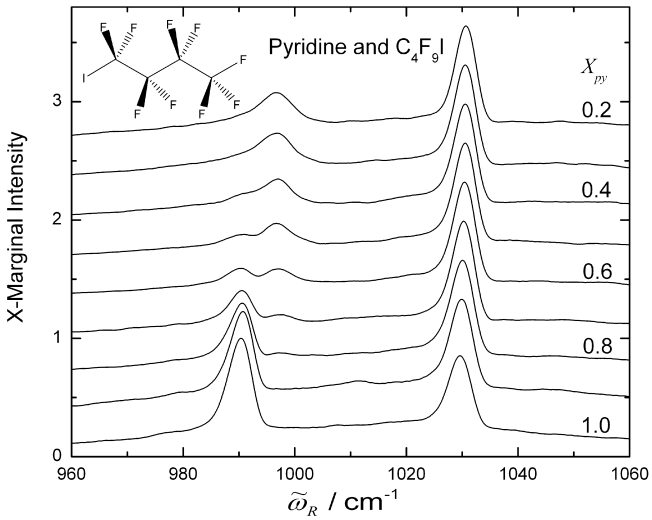

Figure 1. x-Marginal spectra for nine different mole fractions of pyridine in 1-iodo-perfluorobutane. The spectra are normalized to intensity values between zero and unity. The constant offset to the normalized intensity is simply to provide visual clarity among the spectra. The spectra for $X_{py} = 0.5$ shows discernible peaks for both free pyridine and halogen-bonded pyridine. This indicates an equilibrium constant on the order of unity.

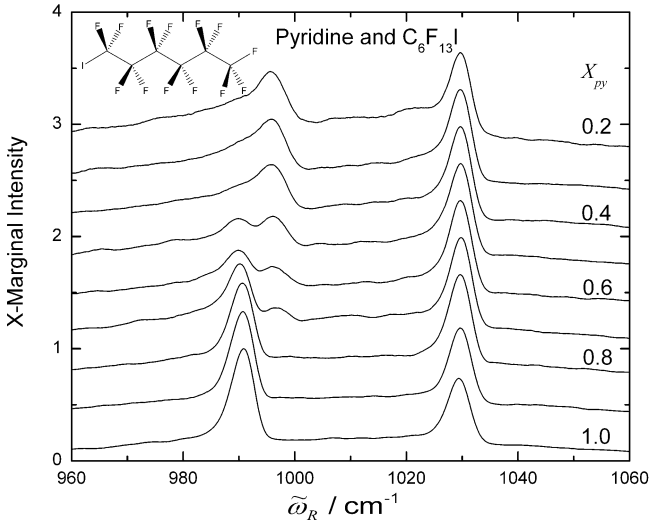

Figure 2. x-Marginal spectra for nine different mole fractions of pyridine in 1-iodo-perfluorohexane. The spectra are normalized to intensity values between zero and unity. The spectra for $X_{py} = 0.5$ shows discernible peaks for both free pyridine and halogen-bonded pyridine. This indicates an equilibrium constant on the order of unity.

exhibits no frequency shift. It is curious, however, that unlike for the case of hydrogen bonding, the ratio of the triangle mode (at ~1030 cm^{-1}) intensity to the ring breathing intensity dramatically increases with halogen bonding. The reason for this is unknown to us but is the subject of current investigations by our group. Table 1 lists a summary of the fitting results for three pyridine/iodo-perfluoroalkanes. There is a very slight mole fraction and temperature dependence on the frequencies of the free and complexed ring breathing mode, so the values reported in Table 1 correspond to a mole fraction of $X_{py} = 0.5$ and a temperature of 20 °C.

Results of the temperature studies are shown in Figures 4, 5, and 6, where $X_{py} = 0.6$ for 1-iodo-perfluorobutane, $X_{py} = 0.5$ for the 1-iodo-perfluorohexane, and $X_{py} = 0.6$ for 2-iodo-perfluoropropane. Shown are x-marginals for several different temperatures spanning over nearly 100 °C. In all three cases,

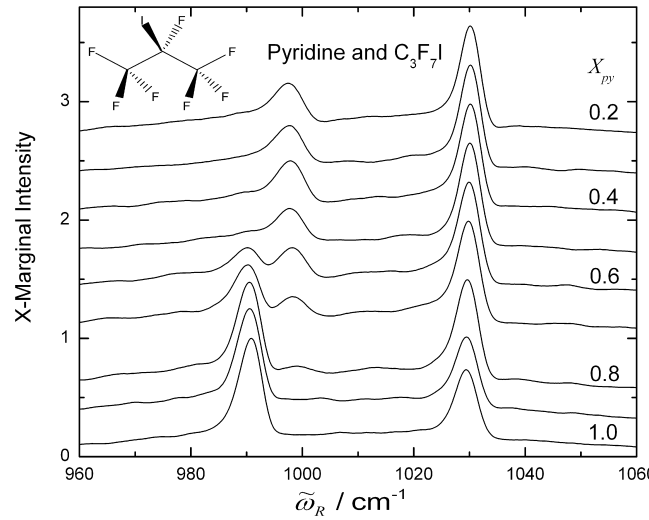

Figure 3. x-Marginal spectra for nine different mole fractions of a pyridine in 2-iodo-perfluoropropane. The spectra are normalized to intensity values between zero and unity. The spectra for $X_{py} = 0.5$ shows no discernible peak for the free pyridine. This implies the equilibrium constant is larger than that for the 1-iodo-perfluoroalkanes.

TABLE 1: Wavenumber Blue Shifts, $\tilde{\Delta}\omega_R$, of the Ring Breathing Mode of Pyridine upon Halogen or Hydrogen Bond Formation[a]

diluent	$\Delta\tilde{\omega}_R$/ cm^{-1}
1-iodo-perfluorobutane	7.8
1-iodo-perfluorohexane	7.6
2-iodo-perfluoropropane	9.7
water[b]	8
formamide[b]	5

[a] The $\tilde{\Delta}\omega_R$ values for the compounds of this work are calculated for a $X_{py} = 0.5$ and $T = 20$ °C based on linear best fits to mole fraction and temperature data. [b] From reference 57.

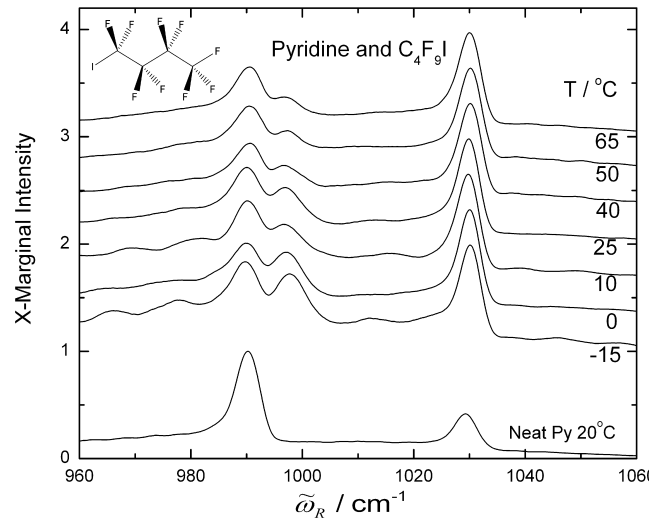

Figure 4. x-Marginal spectra for a $X_{py} = 0.6$ mixture of pyridine and 1-iodo-perfluorobutane collected at several different temperatures. As the temperature is increased, the equilibrium shifts in favor of the free pyridine relative to the halogen bonded complex. This trend with temperature indicates $\Delta^{(1)}H^{\varnothing} < 0$.

the equilibrium shifts toward the halogen bonding complex when temperature is reduced. This shift in equilibrium is more dramatic for the 1-iodo-perfluoroalkanes than for 2-iodo-perfluoropropane.

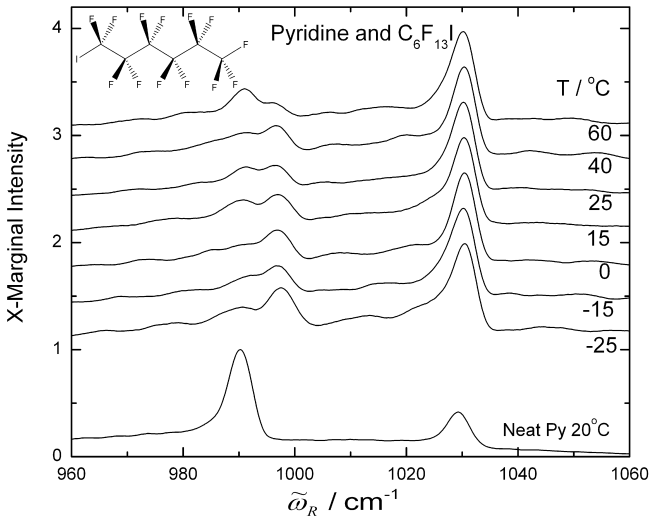

Figure 5. x-Marginal spectra for a $X_{py} = 0.5$ mixture of pyridine and 1-iodo-perfluorohexane collected at several different temperatures. As the temperature is increased, the equilibrium shifts in favor of the free pyridine relative to the halogen bonded complex. This trend with temperature indicates $\Delta^{(1)}H^{\varnothing} < 0$.

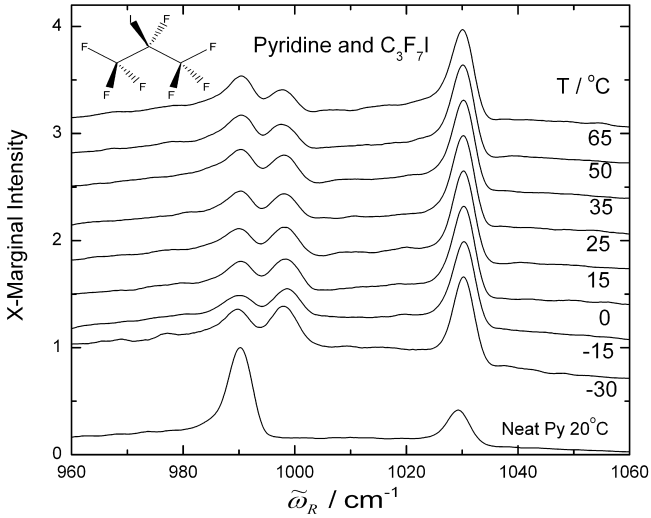

Figure 6. x-Marginal spectra for a $X_{py} = 0.6$ mixture of pyridine and 2-iodo-perfluoropropane collected at several different temperatures. As the temperature is increased, the equilibrium shifts in favor of the free pyridine relative to the halogen bonded complex, but not nearly to the degree for the 1-iodo-perfluoroalkanes. This trend with temperature indicates $\Delta^{(2)}H^{\varnothing} < 0$ but $|\Delta^{(2)}H^{\varnothing}| < |\Delta^{(1)}H^{\varnothing}|$.

VI. Discussion

In principle, the temperature studies should provide quantitative thermodynamic information about the halogen bond formation. Unfortunately, such quantitative information from these data is not reliable for several reasons. First, we are unable to determine the activity coefficients to account for the significant deviations from the Raoult's law reference state. Second, it is reasonable to expect that the electric susceptibility, which gives rise to the $I^{(2)}$ CARS signal, is not the same for the complexed pyridine as the free pyridine. Third, as with all coherent nonlinear optical spectroscopic techniques, it is very difficult to compare absolute signal intensities from one data set to another.

There is a qualitative difference in the x-marginals between the 1-iodo-perfluoroalkanes studied and the 2-iodo-perfluoropropane. The free pyridine peak at 990 cm^{-1} is essentially nonexistent at a mole fraction of $X_{py} = 0.5$ for 2-iodo-perfluoropropane but is clearly present for both of the 1-iodo-perfluoroalkanes (Figures 1−3). This indicates that the equilibrium constant for halogen bond formation between pyridine (py) and the iodo-perfluoroalkane (ipa),

$$\text{py} + \text{ipa} \rightleftharpoons \text{py}\cdots\text{ipa}$$

is large for 2-iodo-perfluoropropane but of order unity for the 1-iodo-perfluoroalkanes.

The Raoult's law reference is used for these binary liquids, and the equation for the equilibrium constant is expressed in terms of mole fraction as

$$K = \frac{X_c}{X_{py}X_{ipa}}$$

where c, py, and ipa stand for the halogen bond complex, free pyridine, and free iodo-perfluoroalkane, respectively. Although one must use caution when comparing equilibrium measurements in these binary systems with those performed at very low concentrations in a neutral diluent, the equilibrium constant of order unity for the 1-iodo-perfluorohexane case is consistent with the very recent ^{19}F NMR measurements of Cabot and Hunter, who also report an equilibrium constant near unity when diluted in both benzene (pK = 0.0) and in CCl_4 (pK = 0.1).[78]

The magnitude of the frequency shift in the ring breathing mode of pyridine is a measure of the energy of the halogen bond between pyridine and the iodo-perfluoroalkane. This contributes to the enthalpy of the halogen bond. However, the overall enthalpy of the halogen bond also includes other factors, such as pryidine−pyridine interaction and iodo-perfluoroalkane−iodo-perfluoroalkane interaction. The similar frequency shift in the ring breathing mode of pyridine upon halogen bonding with all three iodo-perfluoroalkanes suggests comparable enthalpies for all of the iodo-perfluoroalkanes with the enthalpy for 2-iodo-perfluoropropane being slightly more negative than the 1-iodo-perfluoroalkanes. The temperature dependence data shown in Figures 4, 5, and 6 reveal a weaker temperature dependence for 2-iodo-perfluoropropane/pyridine than for the 1-iodo-perfluoroalkanes/pyridine. This implies that the overall enthalpy for the case of 2-iodo-perfluoropropane is small (because $\ln K = -\Delta H^{\varnothing}/RT + \Delta S^{\varnothing}/R$). In summary, the frequency blue shift suggests comparable enthalpies of halogen bond formation, and the temperature study suggests a difference in overall enthalpies for halogen bond formation. This implies some difference in the iodo-perfluoroalkane−iodo-perfluoroalkane interaction for 1-iodoperfluoroalkane as compared to 2-iodoperfluoroalkane. Further, the X-marginal spectra indicate that the equilibrium constant of 2-profluoroalkane/pyridine complex is much larger than that of the 1-iodoperfluoroalkane/pyridine complex. This suggests the difference in the overall entropy contribution to the overall free energy change between 1-iodoperfluoroalkane/pyridine system and 2-iodoperfluoroalkane/pyridine system, as described in the analysis below.

For the overall halogen bonding process, $\Delta^{(x)}G^{\varnothing} = -RT \ln K^{(x)} = \Delta^{(x)}H^{\varnothing} - T\Delta^{(x)}S^{\varnothing}$ where the superscript (x) is 1 for the 1-iodo-perfluoroalkanes and 2 for 2-iodo-perfluoropropane. The temperature studies imply $\Delta^{(2)}H^{\varnothing}$ for 2-iodo-perfluoropropane is less negative than $\Delta^{(1)}H^{\varnothing}$ for the 1-iodo-perfluoroalkanes. The mole fraction studies imply $K^{(2)} > K^{(1)}$; thus, the $T\Delta^{(2)}S^{\varnothing}$ contribution must have a less unfavorable contribution to $\Delta^{(2)}G^{\varnothing}$ than $T\Delta^{(1)}S^{\varnothing}$ does to $\Delta^{(1)}G^{\varnothing}$.

Neither the thermodynamic nor microscopic picture emerging from this study is entirely clear. Nonetheless, taken together, the data presented here lead us to the following hypothesis: *2-Iodo-perfluoropropane has a more ordered liquid structure*

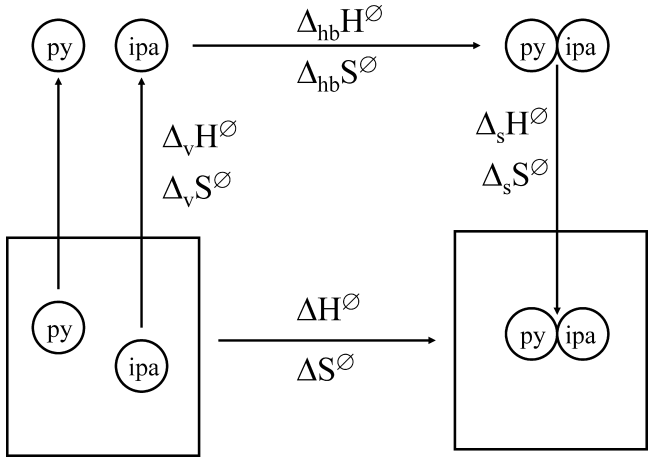

Figure 7. The Hess' law cycle used to interpret the spectroscopic and thermodynamic information about these systems. The overall halogen bonding process is complicated by the fact that it is taking place in the liquid state. Moreover, in these binary liquids, relatively high concentrations of each component are present. This makes it difficult to directly compare thermodynamic results with those obtained from measurements done when the halogen bond participants are highly diluted by a neutral solvent. Here, three basic contributions are considered: solvation of the free components, the halogen bond itself, and solvation of the complex. The spectroscopic information in the form of the blue shift directly probes the halogen bond strength. The temperature studies shown in Figures 4−6 provide information about the overall enthalpy and entropy contributions.

due to the nature and degree of self-halogen bonding than the 1-iodo-perfluoroalkanes at the molecular level. This manifests itself thermodynamically such that 2-iodo-perfluoropropane has both an overall less favorable (but not unfavorable) enthalpic and an overall less unfavorable entropic contribution to the free energy of halogen bonding for the bulk solutions. This ultimately leads to a significantly more favorable free energy for halogen bonding between pyridine and 2-iodo-perfluoropropane versus pyridine and the 1-iodo-perfluoroalkanes. Here, self-halogen bonding means halogen bond formation between the electron-rich fluorine on one iodo-perfluoroalkane molecule and the σ-hole of the iodine on an adjacent iodo-perfluoroalkane molecule of the same type.

There are three main contributors to the overall free energy of halogen bonding for these systems. These are illustrated in Figure 7, which shows the Hess' law cycle used to develop the above hypothesis, as (i) free (nonhalogen bonded to pyridine) iodo-perfluoroalkane and pyridine taken from solution to the vacuum ($\Delta_v^{(x)}H^{\varnothing}$, $\Delta_v^{(x)}S^{\varnothing}$), (ii) gas phase halogen bonding ($\Delta_{hb}^{(x)}H^{\varnothing}$, $\Delta_{hb}^{(x)}S^{\varnothing}$), and (iii) solvation of the halogen bonded complex ($\Delta_s^{(x)}H^{\varnothing}$, $\Delta_s^{(x)}S^{\varnothing}$). As mentioned above, $\Delta_{hb}^{(x)}H^{\varnothing}$ is slightly more negative for 2-iodo-perfluoropropane than for the 1-iodo-perfluoroalkanes, as implied by the blue shift in the ring breathing mode; however, $\Delta_{hb}^{(2)}H^{\varnothing} \simeq \Delta_{hb}^{(1)}H^{\varnothing}$. It also follows for this gas phase reaction that $\Delta_{hb}^{(2)}S^{\varnothing} \simeq \Delta_{hb}^{(1)}S^{\varnothing}$. We take $\Delta_s^{(2)}H^{\varnothing} \simeq \Delta_s^{(1)}H^{\varnothing}$ and $\Delta_s^{(2)}S^{\varnothing} \simeq \Delta_s^{(1)}S^{\varnothing}$ because the pyridine/iodo-perfluoroalkane complex results in an occupied iodine, not allowing for a self-halogen bond interaction. Accepting these arguments as reasonable leaves $\Delta_vH^{\varnothing}$ and $\Delta_vS^{\varnothing}$ to determine the differences in thermodynamic behavior of the 2- versus 1-iodo-perfluoroalkanes. The temperature studies suggest both $\Delta^{(2)}H^{\varnothing}$ and $\Delta^{(1)}H^{\varnothing}$ are negative but $|\Delta^{(2)}H^{\varnothing}| < |\Delta^{(1)}H^{\varnothing}|$. This implies $\Delta_v^{(2)}H^{\varnothing}$ is making a larger positive contribution to the overall enthalpy; hence, $\Delta_v^{(2)}H^{\varnothing} > \Delta_v^{(1)}H^{\varnothing}$. The mole fraction studies suggest $K^{(2)} > K^{(1)}$. Thus, from

$$\ln K^{(2)} > \ln K^{(1)}$$

one sees,

$$\frac{-\Delta^{(2)}H^{\varnothing}}{RT} + \frac{\Delta^{(2)}S^{\varnothing}}{R} > \frac{-\Delta^{(1)}H^{\varnothing}}{RT} + \frac{\Delta^{(1)}S^{\varnothing}}{R}$$

$$T\Delta^{(2)}S^{\varnothing} - T\Delta^{(1)}S^{\varnothing} > \Delta^{(2)}H^{\varnothing} - \Delta^{(1)}H^{\varnothing}$$

Since $\Delta_vH^{\varnothing}$ and $\Delta_vS^{\varnothing}$ determine the difference in thermodynamic behavior,

$$T\Delta_v^{(2)}S^{\varnothing} - T\Delta_v^{(1)}S^{\varnothing} > \Delta_v^{(2)}H^{\varnothing} - \Delta_v^{(1)}H^{\varnothing}$$

and since $\Delta_v^{(2)}H^{\varnothing} > \Delta_v^{(1)}H^{\varnothing}$, the right-hand side is positive. Thus, for the temperatures used in this study, $\Delta_v^{(2)}S^{\varnothing} > \Delta_v^{(1)}S^{\varnothing}$.

These two final inequalities ($\Delta_v^{(2)}H^{\varnothing} > \Delta_v^{(1)}H^{\varnothing} > 0$ and $\Delta_v^{(2)}S^{\varnothing} > \Delta_v^{(1)}S^{\varnothing} > 0$) provide the basis for our conjecture about the molecular level structure. They suggest that there is stronger self-halogen bonding for 2-iodo-perfluoropropane than for the 1-iodo-perfluoroalkanes. At first, there does not appear to be a physically intuitive reason for this conclusion. Perhaps the lone α-fluorine in 2-iodo-perfluoropropane predominately serves as the halogen bond acceptor for the iodine on an adjacent molecule. This could potentially produce an ordered chain. Figure 8 illustrates this idea and the following discussion. The positioning of the iodine and the α-fluorine might work synergistically to produce this chain ordering. It is reasonable that the α-fluorine would be the primary beneficiary of the increased electron density coming from the iodine. This, in turn, would allow the α-fluorine to become a better electron donor

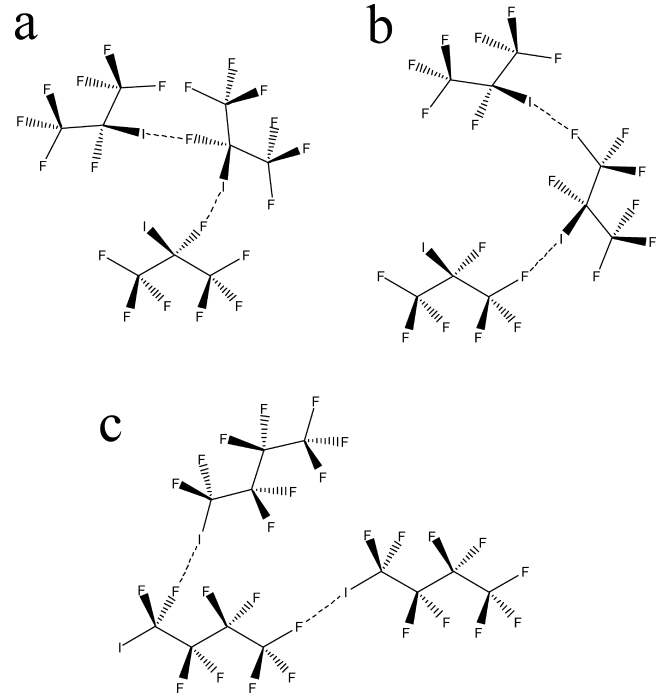

Figure 8. The working hypothesis used to interpret the entirety of the data presented in the current work. For the 2-iodo-perfluoropropane there is (a) relatively stronger α fluorine directed self-halogen bonding than (b) β-based self-halogen bonding. Our hypothesis suggests the I···$^{\alpha}$F is the dominant self-interaction among the 2-iodo-perfluoropropane molecules. (c) There is less significant and less α-directed self-halogen bonding for the 1-iodo-perfluoroalkanes. This leads to a more ordered state for the free (not halogen-bonded to pyridine) 2-iodo-perfluoropropane than for the 1-iodo-perfluoroalkanes. Although speculative, this hypothesis is consistent with the blue shift results, temperature studies, and boiling point information (see text for discussion).

to coordinate with the σ-hole on the adjacent molecule. Thus, most of the self-halogen bonding would be of the I···$^{\alpha}$F type rather than I···$^{\beta}$F.

For the case of the 1-iodo-perfluoroalkanes, the self-halogen bonding would be less directed to the I···$^{\alpha}$F because the two α-fluorines would compete to some degree over the influx of electron density from the iodine. So a small energy difference between I···$^{\alpha}$F and I···$^{\beta}$F combined with the two α fluorine sites that allow for branching of the self-halogen bonding network could conceivably give rise to a higher basal entropy state. This is consistent with both the $\Delta_v^{(2)}H^{\varnothing} > \Delta_v^{(1)}H^{\varnothing} > 0$ and $\Delta_v^{(2)}S^{\varnothing} > \Delta_v^{(1)}S^{\varnothing} > 0$ inequalities.

An important fact about the iodo-perfluoroalkanes which is independent of the $I^{(2)}$ CARS data supports the current hypothesis. It is interesting to consider the boiling points of the iodo-perfluoroalkanes and their simple iodo-alkane counterparts. 2-Iodo-perfluoropropane and 1-iodo-perfluoropropane have essentially the same boiling point (40 and 41 °C, respectively), whereas 2-iodo-propane has a significantly lower boiling point than 1-iodo-propane (89.5 and 102 °C respectively). The simple iodo-alkanes are devoid of self-halogen bonding, and one sees, as expected, that an iodine in the 2 position on propane allows for less effective intermolecular interaction than does an iodine on an iodine at the 1 position. Hence, the boiling point of 2-iodopropane is lower than for 1-iodopropane. Barring any additional interaction, one would expect the 2-iodo-perfluoropropane and the 1-iodo-perfluoropropane to follow the same trend ($T_{boil}^{(2)} < T_{boil}^{(1)}$), but this is not the case. This suggests there must be some additional intermolecular interaction and that it is more significant for 2-iodo-perfluoropropane. Consistent with the proposed hypothesis, this could be self-halogen bonding between the α-fluorine on one 2-iodo-perfluoropropane molecule and the iodine on an adjacent 2-iodo-perfluoropropane.

The clear evidence for relatively strong halogen bonding between pyridine and iodo-perfluoroalkanes suggests that there should be a reasonably strong halogen bond interaction between pyridine and bromo-perfluoroalkanes. Interestingly, pyridine and 1-bromo-perfluorohexane do not mix at room temperature. Additionally, pyridine and perfluorohexane are immiscible at room temperature. These observations suggest that the major driving factor for the miscibility of pyridine and the iodo-perfluoroalkanes is the halogen bond interaction. Further, it suggests the halogen bond interaction between pyridine and bromo-perfluoroalkanes, although likely present, is not sufficient to overcome the generic interactions contributing to the free energy of mixing.

VII. Conclusion

The $I^{(2)}$ CARS study reveals that the halogen bonding between 1-iodo-perfluorobutane, 1-iodo-perfluorohexane, or 2-iodo-perfluoropropane and pyridine is strong. Indeed, peak shifts of around 7−10 cm^{-1} are observed, which is comparable to the ∼8 cm^{-1} shift observed in pyridine/water systems. Despite similar halogen bond strengths between the 1-iodo-perfluoroalkanes/pyridine and the 2-iodo-perfluoropropane/pyridine, qualitatively different thermodynamic behavior is observed. Taken together, these data support the hypothesis that the 1-iodo-perfluoroalkanes and 2-iodo-perfluoropropane have different molecular interactions. A greater degree of self-halogen bonding is believed to be taking place in 2-iodo-perfluoropropane, which leads to a more ordered local molecular structure. Disruption of this ordering provides an increase in entropy that ultimately leads to different equilibrium constants for the overall halogen bonding process in these binary mixtures. The 1-iodo-perfluoroalkane/pyridine systems have equilibrium constants of order unity and the 2-iodo-perfluoropropane/pyridine system has a much larger equilibrium constant.

It is hoped these data and their interpretation presented here might stimulate further study of both halogen bonding to pyridine-based molecules and the potential intermolecular interactions between iodo-perfluoro compounds. Understanding the fundamental dynamics and interactions in iodo-perfluoroalkanes and their mixtures with pyridine is important for applications as varied as crystal engineering and drug design.

From the experimental point of view, more traditional vibrational spectroscopy than $I^{(2)}$ CARS, such as conventional Raman and FTIR, is an obvious direction. Ultraviolet spectroscopy has been employed to identify halogen bonding[79] and will be an avenue for further study, as well. Beyond that, perhaps studies on clusters of these systems could provide additional insight and serve as an empirical bridge between full liquid phase behavior and small cluster properties gleaned from computational studies. This has been done for hydrogen bonding systems.[80]

To our knowledge, the behavior of the α and β fluorines have not been explored via computational chemistry. This could provide insight into the idea of self-halogen bonding proposed in the current work and perhaps even on its contribution to the thermodynamic properties of the iodo-perfluoroalkanes.

Acknowledgment. This work was supported by NSF CAREER Grant CHE-0341087, the Dreyfus Foundation, and the Concordia College Chemistry Research Endowment.

References and Notes

(1) Metrangolo, P.; Resnati, G., *Halogen Bonding: Fundamentals and Applications*; Springer: Berlin, 2008.
(2) Metrangolo, P.; Neukirch, H.; Pilati, T.; Resnati, G. *Acc. Chem. Res.* **2005**, *38*, 386.
(3) Auffinger, P.; Hays, F. A.; Westhof, E.; Shing Ho, P. *Proc. Natl. Acad. Sci.* **2004**, *101*, 16789.
(4) Politzer, P.; Lane, P.; Concha, M.; Ma, Y.; Murray, J. S. *J. Mol. Model.* **2007**, *13*, 305.
(5) Clark, T.; Hennemann, M.; Murray, J. S.; Polizter, P. *J. Mol. Model.* **2007**, *13*, 291.
(6) Mohajeri, A.; Pakiari, A. H.; Bagheri, N. *Chem. Phys. Lett.* **2009**, *467*, 393.
(7) Murray, J. S.; Lane, P.; Politzer, P. *J. Mol. Model.* **2009**, *15*, 723.
(8) Murray, J. S.; Lane, P.; Politzer, P. *Int. J. Quantum Chem.* **2007**, *107*, 2286.
(9) Politzer, P.; Murray, J. S.; Lane, P. *Int. J. Quantum Chem.* **2007**, *107*, 3046.
(10) Murray, J. S.; Lane, P.; Clark, T.; Politzer, P. *J. Mol. Model.* **2007**, *13*, 1033.
(11) Guthrie, F. *J. Chem. Soc.* **1863**, *16*, 239.
(12) Remsen, I.; Norris, J. F. *Am. Chem. J.* **1896**, *18*, 90.
(13) Hassel, O.; Hvoslef, J. *Acta Chem. Scand.* **1954**, *8*, 873.
(14) Hassel, O.; Stromme, K. O. *Acta Chem. Scand.* **1959**, *13*, 275.
(15) Groth, P.; Hassel, O. *Acta Chem. Scand.* **1964**, *18*, 402.
(16) Hassel, O. *Science* **1970**, *170*, 497.
(17) Bent, H. A. *Chem. Rev.* **1968**, *68*, 587.
(18) Bernard-Houplain, M.-C.; Belanger, G.; Sandorfy, C. *J. Chem. Phys.* **1972**, *57*, 530.
(19) Bernard-Houplain, M.-C.; Sandorfy, C. *J. Chem. Phys.* **1972**, *56*, 3412.
(20) Paolo, T. D.; Sandorfy, C. J. *Can. J. Chem.* **1974**, *52*, 3612.
(21) Paolo, T. D.; Sandorfy, C. J. *Chem. Phys. Lett.* **1974**, *26*, 466.
(22) Ramasubbu, N.; Parthasarathy, R.; Murray-Rust, P. *J. Am. Chem. Soc.* **1986**, *108*, 4308.
(23) Murray-Rust, P.; Stalling, W. C.; Monti, C. T.; Preston, R. K.; Glusker, J. P. *J. Am. Chem. Soc.* **1983**, *105*, 3206.
(24) Murray-Rust, P.; Motherwell, W. D. S. *J. Am. Chem. Soc.* **1979**, *101*, 4374.
(25) Riley, K. E.; Murray, J. S.; Polizer, P.; Concha, M. C.; Hobza, P. *J. Chem. Theory Comput.* **2009**, *5*, 155.
(26) Metrangolo, P.; Resnati, G. *Chem.—Eur. J.* **2001**, *7*, 2511.
(27) Metrangolo, P.; Panzeri, W.; Recupero, F.; Resnati, G. *J. Fluorine Chem.* **2002**, *114*, 27.

(28) Valerio, G.; Raos, G.; Meille, S. V.; Metrangolo, P.; Resnati, G. *J. Phys. Chem. A* **2000**, *104*, 1617.
(29) Messina, M. T.; Metrangolo, P.; Panseri, W.; Pilati, T.; Resnati, G. *Tetrahedron* **2001**, *57*, 8543.
(30) Fox, D. B.; Liantonio, R.; Metrangolo, P.; Pilati, T.; Resnati, G. *J. Fluorine Chem.* **2004**, *125*, 271.
(31) Metrangolo, P.; Resnati, G.; Pilati, T.; Liantonio, R.; Meyer, F. *J. Polym. Sci., Part A: Polym. Chem.* **2007**, *45*, 1.
(32) Metrangolo, P.; Meyer, F.; Pilati, T.; Proserpio, D. M.; Resnati, G. *Cryst. Growth Des.* **2008**, *8*, 654.
(33) Lu, X.-Y.; Zou, J.-W.; Wang, J.-H.; Jiang, Y.-J.; Yu, Q.-S. *J. Phys. Chem. A* **2007**, *111*, 10781.
(34) Riley, K. E.; Merz, K. M., Jr. *J. Phys. Chem. A* **2007**, *111*, 1688.
(35) Riley, K. E.; Hobza, P. *J. Chem. Theory Comput.* **2008**, *4*, 232.
(36) Lommerse, J. P. M.; Stone, A. J.; Taylor, R.; Allen, F. H. *J. Am. Chem. Soc.* **1996**, *118*, 3108.
(37) Aakeröy, C. B.; Fasulo, M.; Schultheiss, N.; Desper, J.; Moore, C. *J. Am. Chem. Soc.* **2007**, *129*, 13772.
(38) Beauchamp, G. *J. Phys. Chem. A* **2008**, *112*, 10674.
(39) Goroff, N. S.; Curtis, S. M.; Webb, J. A.; Fowler, F. W.; Lauher, J. W. *Org. Lett.* **2005**, *7*, 1981.
(40) Mukai, T.; Nishikawa, K. *Chem. Lett.* **2009**, *38*, 402.
(41) Triguero, S.; Llusar, R.; Polo, V.; Fourmigué, M. *Cryst. Growth. Des.* **2008**, *8*, 2241.
(42) Nguyen, H. L.; Horton, P. N.; Hursthouse, M. B.; Legon, A. C.; Bruce, D. W. *J. Am. Chem. Soc.* **2004**, *126*, 16.
(43) Metrangolo, P.; Meyer, F.; Pilati, T.; Proserpio, D. M.; Resnati, G. *Cryst. Growth Des.* **2008**, *8*, 654.
(44) Shirman, T.; Lamere, J.-F.; Shimon, L.; Gupta, T.; Martin, J. M. L.; van der Boom, M. E. *Cryst. Growth Des.* **2008**, *8*, 3066.
(45) Voth, A. R.; Hays, F. A.; Ho, P. S. *Proc. Nat. Acad. Sci.* **2007**, *104*, 6188.
(46) Tawarada, R.; Seio, K.; Sekine, M. *J. Org. Chem.* **2008**, *73*, 383.
(47) Lu, Y.; Shi, T.; Wang, Y.; Yang, H.; Yan, X.; Luo, X.; Jiang, H.; Zhu, W. *J. Med. Chem.* **2009**, *52*, 2854.
(48) Liu, L.; Baase, W. A.; Matthews, B. W. *J. Mol. Biol.* **2009**, *385*, 595.
(49) Gopalakrishnan, B.; Aparna, V.; Jeevan, J.; Ravi, M.; Desiraju, G. R. *J. Chem. Inf. Model.* **2005**, *45*, 1101.
(50) Himmel, D. M.; Das, K.; Clark, A. D., Jr.; Hughes, S. H.; Benjahad, A.; Oumouch, S.; Guillemont, J.; Coupa, S.; Poncalet, A.; Csoka, I.; Meyer, C.; Andries, K.; Nguyen, C. H.; Grierson, D. S.; Arnold, E. *J. Med. Chem.* **2005**, *48*, 7582.
(51) Jiang, Y.; Alcaraz, A. A.; Chen, J.; Kobayashi, H.; Lu, Y. J.; Snyder, J. P. *J. Med. Chem.* **2006**, *49*, 1891.
(52) Schlücker, S.; Singh, R. K.; Asthana, B. P.; Popp, J.; Kiefer, W. *J. Phys. Chem.* **2001**, *105*, 9983.
(53) Asthana, B. P.; Takahashi, H.; Kiefer, W. *Chem. Phys. Lett.* **1983**, *94*, 41.
(54) Kreyenschimdt, M.; Eysel, H. H.; Asthana, B. P. *J. Raman Spectrosc.* **1993**, *24*, 645.
(55) Deckert, V.; Asthana, B. P.; Mishra, P. C.; Kiefer, W. *J. Raman Spectrosc.* **1996**, *27*, 907.
(56) Schlücker, S.; Heid, M.; Singh, R. K.; Asthana, B. P.; Popp, J.; Kiefer, W. *Z. Phys. Chem.* **2002**, *216*, 217.
(57) Berg, E. R.; Freeman, S. A.; Green, D. D.; Ulness, D. J. *J. Phys. Chem. A* **2006**, *110*, 1684.
(58) Berg, E. R.; Green, D. D.; Moliva, D. C.; Bjerke, B. T.; Gealy, M. W.; Ulness, D. J. *J. Phys. Chem. A.* **2008**, *112*, 833.
(59) Dugan, M. A.; Mellinger, J. S.; Albrecht, A. C. *Chem. Phys. Lett.* **1988**, *147*, 411.
(60) Dugan, M. A.; Albrecht, A. C. *Phys. Rev. A* **1991**, *43*, 3877.
(61) Dugan, M. A.; Albrecht, A. C. *Phys. Rev. A* **1991**, *43*, 3922.
(62) Schaertel, S. A.; Albrecht, A. C.; Lau, A.; Kummrow, A. *Appl. Phys. B: Laser Opt.* **1994**, *59*, 377.
(63) Schaertel, S. A.; Lee, D.; Albrecht, A. C. *J. Raman Spectrosc.* **1995**, *59*, 889.
(64) Kozich, V. P.; Lau, A.; Pfeiffer, M.; Kummrow, A. *J. Raman Spectrosc.* **1999**, *30*, 473.
(65) Lau, A.; Kummrow, A.; Pfeiffer, M.; Woggon, S. *J. Raman Spectrosc.* **1994**, *25*, 607.
(66) Stimson, M. J.; Ulness, D. J.; Albrecht, A. C. *Chem. Phys. Lett.* **1996**, *263*, 185.
(67) Ulness, D. J.; Kirkwood, J. C.; Stimson, M. J.; Albrecht, A. C. *J. Chem. Phys.* **1997**, *107*, 7127.
(68) Ulness, D. J.; Stimson, M. J.; Albrecht, A. C. *Chem. Phys.* **1997**, *222*, 17.
(69) Ulness, D. J. *J. Phys. Chem. A* **2003**, *107*, 8111.
(70) Aung, P. P.; Cosert, K. M.; Weisel, L. R.; Schulz, T. F.; Gealy, M. W.; Ulness, D. J. *J. Raman Spectrosc.* **2005**, *36*, 409.
(71) Weisel, L. R.; Ta, T.; Booth, E. C.; Ulness, D. J. *J. Raman Spectrosc.* **2007**, *38*, 11.
(72) Gladysz, J. A., Cuwar, D. P., Horváth, I. T., Eds.; *Handbook of Fluorous Chemistry*; Wiley−VCH, Verlag, Gmblt and Co.: Weinheim, Germany, 2004.
(73) Gladysz, J. A. *Science* **1994**, *266*, 55.
(74) Horváth, I. T.; Rádai, J. *Science* **1994**, *266*, 72.
(75) Reed, A. E.; Curtiss, L. A.; Weinhold, F. *Chem. Rev.* **1988**, *88*, 899.
(76) Press, W. H.; Flannery, B. P.; Teukolsky, S. A.; Vetterling, W. T. *Numerical Recipes in C: The Art of Scientific Computing*, 2nd ed.; Cambridge University Press: New York, 1992.
(77) Wolfram, S. *Mathematica 3.0 Standard Add-on Packages*; Cambridge University Press: New York, 1996.
(78) Cabot, R.; Hunter, C. A. *Chem. Commun.* **2009**, 2005.
(79) Zou, W. S.; Han, J.; Jin, W. J. *J. Phys. Chem. A* **2009**, *113*, 10125.
(80) Wakisaka, A.; Abdoul-Carime, H.; Yamamoto, Y.; Kiyozumi, Y. *J. Chem. Soc. Faraday Trans.* **1998**, *94*, 369.

JP9057127